resonance at room temperature centered about a g value of 1.996 with no resolvable hyperfine coupling and a peak to peak width of 28 G. Similar spectra have been reported for $Ru(bpy)(DBSQ)_2^+$ and $Ru(py)_2(DBSQ)_2^+$.[11] The related Ru(III) complex containing a single $Phenox^-$ radical ligand, $Ru(PPh_3)_2(Cl)_2(Phenox)$, is diamagnetic and shows a sharp NMR spectrum.

When the reaction between HPhenox and $Ru(PPh_3)_3Cl_2$ was carried out in air, the product obtained was the neutral $Ru(PPh_3)Cl(Phenox)(oxPhenox)$ molecule shown in Figure 1.[12] The oxidized Phenox ligand (III, oxPhenox) contains two chiral carbon

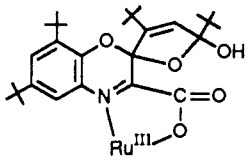

III

centers, and the metal center of the complex is also chiral. Strong magnetic coupling between the remaining Phenox radical and the Ru(III) center results in overall diamagnetism for the complex. NMR spectra indicate that $Ru(PPh_3)Cl(Phenox)(oxPhenox)$ is obtained exclusively as the diastereomer shown in Figure 1.

The mechanism of oxidation of the coordinated $Phenox^-$ ligand is pertinent to mechanistic models for both oxygenase and dioxygenase metalloenzymes. We belive that the initial step in the process is coordination and one-electron reduction of molecular oxygen at a vacant site of the Ru(II) form of the complex (Scheme I, part A). A vacancy in the Ru(II) coordination sphere may be created by dissociation of the chloro ligand; indirect evidence for this is seen in the change in stereochemistry of the complex, from cis to trans. The coordinated superoxide radical may then add to the Phenox ring at the radical carbon atom. The succeeding steps in oxygen atom rearrangement remain unclear, but appear to follow a mechanism that is similar to that of the extradiol dioxygenases.[13] The result is addition of two oxygen atoms across the C1-C2 bond of the ring to give a coordinated carboxylic acid and a conjugated ketone. Protocatechuate-4,5-dioxygenase and catechol-2,3-dioxygenase both catalyze the addition of two oxygen atoms of dioxygen across an outer carbon-carbon bond of catechol to give an aldehyde-carboxylic acid in a reaction that appears to occur at an iron center of the enzyme.[13] Addition of a second molecule of dioxygen at the ketonic carbon center is thought to occur next,[14] with cyclization of the ketonic oxygen to form the dihydrofuran ring (Scheme I, part B). In a subsequent step, one oxygen atom of the bound peroxo group is abstracted by triphenylphosphine in a reaction that parallels iron abstraction of oxygen from the 4a peroxo group of the oxygenated dihydropterin of PAH.[1] Protonation of the remaining oxo anion gives the coordinated oxPhenox ligand. From the structure of *trans*-$Ru(PPh_3)Cl(Phenox)(oxPhenox)$ it appears that dioxygen addition to the ketonic carbon occurs selectively at the side of the complex away from the bulky phosphine. Cyclization is directed by the steric interactions between *tert*-butyl groups of the dihydrofuran ring and the phosphine phenyl rings.

Oxygen addition to the Ru(II)-$Phenox^-$ unit may parallel oxygen binding to the Cu(I)-reduced pterin center of the bacterial PAH. Both reactions involve one-electron oxidation of the metal, with additional charge required for dioxygen activation provided by a reduced ligand. However, the 2-aminopyrimidone ring of the pterin cofactor provides protection against oxidation, and oxygen transfer occurs to substrate. The phenoxazenylate radical and also the catecholate ring, in the case of the catechol dioxygenase, lack this protection and are themselves oxidized.

Acknowledgment. We gratefully acknowledge the help of Dr. Anthony Spek with solution of the $Ru(PPh_3)(Cl)(Phenox)(oxPhenox)$ crystal structure and Professor David Walba and Dr. Anthony Arduango for providing helpful comments on the oxidation mechanism. This research was supported by the National Science Foundation (Grant No. CHE-88-09923); ruthenium trichloride was provided by Johnson Matthey, Inc., through their Metal Loan Program.

Supplementary Material Available: Tables giving crystal data and details of the structure determination, anisotropic thermal parameters, hydrogen atom locations, and bond lengths and angles for $Ru(PPh_3)Cl(Phenox)(oxPhenox)$ (15 pages); observed and calculated structure factors for $Ru(PPh_3)Cl(Phenox)(oxPhenox)$ (23 pages). Ordering information is given on any current masthead page.

(11) (a) Lever, A. B. P.; Auburn, P. R.; Dodsworth, E. S.; Haga, M.; Liu, W.; Melnik, M.; Nevin, W. A. *J. Am. Chem. Soc.* **1988**, *110*, 8076. (b) Lever, A. B. P.; Auburn, P. R.; Dodsworth, E. S.; Haga, M.; Nevin, W. A., to be submitted for publication.

(12) Synthesis of $Ru(PPh_3)Cl(Phenox)(oxPhenox)$: An ethanol solution (50 mL) containing 260 mg (0.26 mmol) of $Ru(PPh_3)_3Cl_2$ and 280 mg (0.66 mmol) of HPhenox was gently refluxed in air for 4 h. The resulting blue-green solution was filtered to remove unreacted starting material and reduced in volume to give a dark green precipitate. The crude product was separated from solution by filtration and recrystallized from a dichloromethane/hexane solution. Yield: 220 mg (63%). *tert*-Butyl resonances appear in the NMR spectrum for the complex at 0.78, 0.81, 1.04, 1.23, 1.39, 1.42, 1.47, and 1.63 ppm. X-ray analysis of $Ru(PPh_3)(Cl)(Phenox)(oxPhenox)$: monoclinic, space group $P2_1/c$, a = 19.092 (6) Å, b = 16.018 (7) Å, c = 24.889 (10) Å, β = 111.74 (3)°, V = 7070 (5) Å^3, Z = 4, R = 0.060 for 3679 unique observed reflections. Details of the structure determination are given with the supplementary material.

(13) Arciero, D. M.; Lipscomb, J. D. *J. Biol. Chem.* **1986**, *261*, 2170.

(14) Since the ketonic carbon atom is less nucleophilic than other sites on the opened ring, initial oxygen attack may occur elsewhere with subsequent transfer to this atom. To give the observed stereochemistry, attack and migration must occur at the face of the partially oxidized Phenox ligand that is opposite from the triphenylphosphine.

Formation and Properties of a $NiFe_3S_4$ Cluster in *Pyrococcus furiosus* Ferredoxin

Richard C. Conover, Jae-Bum Park, Michael W. W. Adams, and Michael K. Johnson*

School of Chemical Sciences and Center for Metalloenzyme Studies University of Georgia, Athens, Georgia 30602

Received December 26, 1989

The NiFe-enzyme CO dehydrogenase (or acetyl-CoA synthase) catalyzes CO oxidation in vitro and the formation of a carbon-carbon bond in vivo. EPR studies of the enzyme from the acetogen *Clostridium thermoaceticum*[1] and from the methanogen *Methanosarcina thermophila*[2] have provided evidence for a CO-binding, NiFe-containing catalytic site, in addition to multiple Fe-S clusters. Although the stoichiometry of the novel mixed-metal center is unknown, EXAFS studies indicate substantial S ligation at the Ni.[3] A second type of CO dehydrogenase, which catalyzes only CO oxidation, is found in the photosynthetic bacterium *Rhodospirillum rubrum*. Recent EPR studies of this enzyme also indicate a mixed Ni- and Fe-containing center as the site of CO activation, although the spectroscopic properties of this center are quite distinct from those of other CO dehydrogenases.[4] Since these studies suggest that CO activation by these enzymes occurs at a novel Ni-Fe-S center and synthetic model compounds are not available, we have initiated a program to investigate the properties of cubane-type $[NiFe_3S_4]$ clusters. Here we report

* Corresponding author. Department of Chemistry, University of Georgia, Athens, GA 30602.

(1) (a) Ragsdale, S. W.; Wood, H. G.; Antholine, W. E. *Proc. Natl. Acad. Sci. U.S.S.* **1985**, *82*, 6811-6814. (b) Ragsdale, S. W.; Ljungdahl, L. G.; DerVartanian, D. V. *Biochem. Biophys. Res. Commun.* **1983**, *115*, 658-665.

(2) Terlesky, K. C.; Barber, M. J.; Aceti, D. J.; Ferry, J. G. *J. Biol. Chem.* **1987**, *262*, 15392-15395.

(3) (a) Cramer, S. P.; Eidsness, M. K.; Pan, W.-H.; Morton, T. A.; Ragsdale, S. W.; DerVartanian, D. V.; Ljungdahl, L. G.; Scott, R. A. *Inorg. Chem.* **1987**, *26*, 2477-2479. (b) Bastian, N. R.; Diekert, G.; Niederhoffer, E. C.; Teo, B.-K.; Walsh, C. T.; Orme-Johnson, W. H. *J. Am. Chem. Soc.* **1988**, *110*, 5581-5582.

(4) Stephens, P. J.; McKenna, M.-C.; Ensign, S. A.; Bonam, D.; Ludden, P. A. *J. Biol. Chem.* **1989**, *264*, 16347-16350.

0002-7863/90/1512-4562$02.50/0

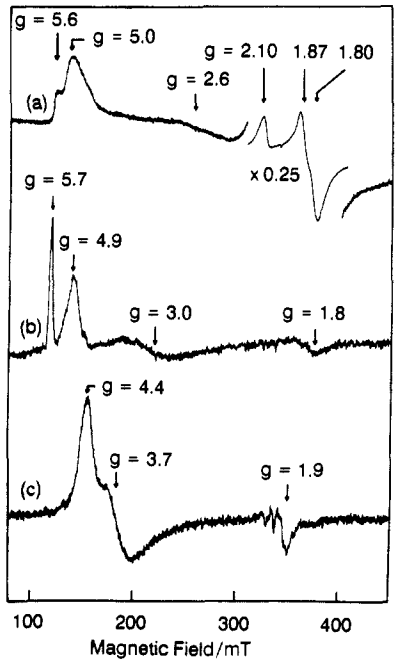

Figure 1. X-band EPR spectra of dithionite-reduced *P. furiosus* Fd containing a $[Fe_4S_4]^+$ cluster (a), a $[NiFe_3S_4]^+$ cluster (b), and a cyanide-bound $[NiFe_3S_4]^+$ cluster (c): (a) 0.5 mM Fd in 50 mM Tris·HCl buffer, pH 7.8; microwave power, 10 mW; temperature, 8 K; (b) 0.3 mM Fd in 100 mM Mes buffer, pH 6.0; microwave power, 50 mW; temperature, 4.5 K; (c) 0.25 mM Fd and 12.5 mM potassium cyanide in 100 mM Mes buffer, pH 6.0; microwave power, 1 mW; temperature, 7 K. All spectra were recorded at 9.49 GHz with 0.63-mT modulation amplitude.

evidence for the formation of a $[NiFe_3S_4]^+$ center in *Pyrococcus furiosus* ferredoxin (Fd) and EPR characterization of the ground-state properties of this novel mixed-metal cluster. Moreover, EPR studies indicate that the Ni site is capable of binding cyanide, a potent inhibitor of all known CO dehydrogenases.[5]

P. furiosus Fd is a monomeric protein, M_r = 7500, containing a single $[Fe_4S_4]$ cluster when isolated under anaerobic conditions in the presence of sodium dithionite.[6,7] The amino acid sequence shows three cysteine residues (Cys 11, 17, and 56) in an arrangement typical of that found in bacterial 4Fe ferredoxins, but an aspartate residue (Asp 14) replaces the fourth cysteine residue that would normally complete the cluster coordination.[7] Non-cysteinyl (aspartate and/or OH^-) ligation of one Fe is manifest in the novel spectroscopic properties of the $[Fe_4S_4]^{2+,+}$ cluster and the ease of quantitative removal of this Fe atom under oxidizing conditions to yield a conventional $[Fe_3S_4]^{+,0}$ cluster.[8]

The procedure used in forming a $[NiFe_3S_4]$ cluster in *P. furiosus* Fd was similar to those described by Münck and co-workers for incorporating Zn(II) and Co(II) into the Fe_3S_4 core of *Desulfovibrio gigas* FdII to give $[ZnFe_3S_4]$ and $[CoFe_3S_4]$ clusters.[9] The dithionite-reduced $[Fe_3S_4]$ form of *P. furiosus* Fd in 100 mM Mes buffer, pH 6.0, was incubated anaerobically with a 20-fold excess of $Ni(NO_3)_2$ for 15 min at room temperature. Excess Ni^{2+} was removed by treatment with 25 mM EDTA followed by gel filtration using Sephadex G-25 under anaerobic conditions. Metal analyses using plasma emission spectroscopy indicated 3.3 ± 0.3 Fe atoms and 1.4 ± 0.2 Ni atoms per molecule.

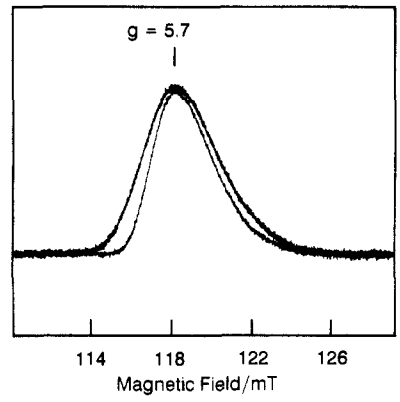

Figure 2. ^{61}Ni broadening of the low-field EPR resonance of *P. furiosus* $[NiFe_3S_4]^+$ Fd. The inner trace is for a sample prepared with natural-abundance Ni, and the outer trace is for the ^{61}Ni-labeled sample. The samples were both 0.35 mM in Fd in 100 mM Mes buffer, pH 6.0. Conditions: microwave power, 50 mW; temperature, 4.5 K; microwave frequency, 9.42 GHz; modulation amplitude, 0.63 mT.

Figure 1 shows X-band EPR spectra of the dithionite-reduced *P. furiosus* Fd containing the native $[Fe_4S_4]^+$ center[10] and the proposed $[NiFe_3S_4]$ cluster in the absence and presence of a 50-fold excess of potassium cyanide. In each case the spectrum is dominated by a different $S = {}^3/_2$ species, indicating that Ni(II) incorporation into the $[Fe_3S_4]^0$ center is accompanied by a further one-electron reduction to yield a stable $S = {}^3/_2$ $[NiFe_3S_4]^+$ cluster. The observed g values of each $S = {}^3/_2$ species are readily rationalized in terms of the appropriate spin Hamiltonian, $\hat{H}_e$, with an isotropic g tensor, g_0:

$$\hat{H}_e = D\left[S_z^2 - \frac{15}{12} + (E/D)(S_x^2 - S_y^2)\right] + g_0\beta\mathbf{H}\cdot\mathbf{S} \quad (1)$$

where D and E are the axial and rhombic zero field splitting parameters, respectively.

Variable-temperature EPR studies have facilitated analysis of the spectrum for the $[Fe_4S_4]^+$ Fd, Figure 1a, in terms of a spin mixture of a $S = {}^1/_2$ species (~20%), g = 2.10, 1.87, 1.80, and a $S = {}^3/_2$ species (~80%) that is subject to a zero-field splitting of 7.0 ± 0.4 cm^{-1}.[8] The resonance at g = 5.6 and the resonances at 5.0 and 2.6 arise from the upper and lower Kramers doublets, respectively, and these g values are very close to the low-field effective g values predicted by eq 1 with E/D = 0.22, g_0 = 1.98, and D = +3.3 ± 0.2 cm^{-1}.[8]

The EPR spectrum of the $[NiFe_3S_4]^+$ Fd, Figure 1b, comprises positive maxima at g = 5.7 and 4.9, a broad derivative centered at g = 2.9, and a weak negative feature at g = 1.8 that are interpretable entirely in terms of a $S = {}^3/_2$ ground state. For example, for E/D = 0.18 and g_0 = 2, eq 1 predicts g_x = 2.88, g_y = 4.95, and g_z = 1.84 for one doublet and g_x = 1.12, g_y = 0.94, and g_z = 5.82 for the other doublet. The temperature dependence of the low-field EPR signals (data not shown) reveals that the g = 5.7 and 4.9 components originate from the lower and upper doublets, respectively. Hence, the zero-field splitting is opposite in sign compared to the $S = {}^3/_2$ $[Fe_4S_4]^+$ center, and analysis of the relative intensity of the g = 5.8 and g = 4.9 features as a function of $1/T$ indicate that D = −2.2 ± 0.2 cm^{-1}. Confirmatory evidence that the changes in the EPR characteristics arise from Ni insertion to yield a $[NiFe_3S_4]^+$ cluster is provided by the 0.6-mT broadening of the g = 5.7 feature in the ^{61}Ni-labeled sample; see Figure 2. Moreover, these EPR characteristics do not appear to be unique to a $[NiFe_3S_4]^+$ cluster in *P. furiosus* Fd. After completion of this work, we became aware that analogous low-field EPR resonances have been observed by Münck and co-workers in their attempts to form a $[NiFe_3S_4]$ cluster in *D. gigas* FdII.[11]

(5) Ensign, S. A.; Hyman, M. R.; Ludden, P. W. *Biochemistry* **1989**, *28*, 4973–4979.
(6) Aono, S.; Bryant, F. O.; Adams, M. W. W. *J. Bacteriol.* **1989**, *171*, 3433–3439.
(7) Howard, J. B.; Eccleston, E.; Park, J.-B.; Adams, M. W. W., manuscript in preparation.
(8) Conover, R. C.; Kowal, A. T.; Fu, W.; Park, J.-B.; Aono, S.; Adams, M. W. W.; Johnson, M. K. *J. Biol. Chem.*, in press.
(9) (a) Moura, I.; Moura, J. J. G.; Münck, E.; Papaefthymiou, V.; LeGall, J. *J. Am. Chem. Soc.* **1986**, *108*, 349–351. (b) Surerus, K. K.; Münck, E.; Moura, I.; Moura, J. J. G.; LeGall, J. *J. Am. Chem. Soc.* **1987**, *109*, 3805–3807.
(10) The EPR spectrum shown for the $[Fe_4S_4]^+$ form is that of the anaerobically isolated Fd. However, identical spectra were obtained for samples prepared in the same way as the $NiFe_3S_4$ Fd with Fe(II) in place of Ni(II).
(11) Surerus, K. K. Ph.D. Dissertation, 1989, University of Minnesota.

Strong evidence for cyanide binding at the Ni site is provided by the complete conversion of the $S = {}^3/_2$ $[NiFe_3S_4]^+$ EPR spectrum to a new resonance, $g = 4.4$, 3.7, and 1.9, on addition of a 50-fold excess of potassium cyanide, Figure 1c. In contrast, the EPR and low-temperature magnetic circular dichroism spectra of the $S = {}^3/_2$ $[Fe_4S_4]^+$ centers in this Fd were unaffected by the addition of a 50-fold excess of potassium cyanide (data not shown). The g values of the cyanide-bound $[NiFe_3S_4]^+$ cluster are indicative of an axial $S = {}^3/_2$ species ($E/D = 0.06$), and temperature-dependence studies (4-15 K) show that this resonance arises exclusively from the lower Kramers doublet, i.e., $D > 0$.

On the basis of the available spectroscopic data, it is not possible at the present time to determine if a similar $[NiFe_3S_4]^+$ cluster constitutes the active site of CO dehydrogenases. Ill-defined $S = {}^3/_2$ EPR signals centered around $g = 5$ are apparent in both dithionite- and CO-reduced samples of *C. thermoaceticum* CO dehydrogenase,[12] in addition to the novel $S = {}^1/_2$ resonance, $g_\parallel = 2.03$ and $g_\perp = 2.07$, that is only observed on CO reduction.[1] Moreover, it is important to note that the $S = {}^1/_2$ resonance is a relatively minor component, typically accounting for 0.15 spins/Ni.[12] EPR signals near $g = 4.3$ from a $S > {}^1/_2$ center as well as a $S = {}^1/_2$ resonance, $g = 2.04$, 1.90, and 1.71, have been assigned to the NiFe center in *R. rubrum* CO dehydrogenase.[4] Clearly, the results reported herein call for more detailed characterization of the low-field EPR signals in CO dehydrogenases. The spectroscopic consequences of binding other ligands, including CO, to the $[NiFe_3S_4]^+$ cluster in *P. furiosus* Fd are currently under investigation in this laboratory.

Acknowledgment. This work was supported by the NSF (DMB8796212 to M.K.J. and DMB8805255 to M.W.W.A.), the NIH (GM33806 to M.K.J.), and the DOE (FG09-88ER13901 to M.W.W.A.). We thank Drs. Eckard Münck and Kristene Surerus for informing us of the results of attempts to form a $[NiFe_3S_4]$ cluster in *D. gigas* FdII and Dr. Stephen Ragsdale for informing us of EPR results on *C. thermoaceticum* CO dehydrogenase prior to publication.

Registry No. CO, 630-08-0; CO dehydrogenase, 64972-88-9; acetyl-CoA synthase, 9012-31-1.

(12) (a) Zambrano, I. C. Ph.D. Dissertation, 1986, Louisiana State University. (b) Lindahl, P. A.; Münck, E.; Ragsdale, S. W. *J. Biol. Chem.* **1990**, *265*, 3873-3879.

Reduction of an Electronically Unsaturated Transition-Metal η^2-Acyl Complex. Arene Formation from Deoxygenative Acyl Coupling with a Cyclopentadienyl Ligand

Tara Y. Meyer and Louis Messerle*

Department of Chemistry, The University of Iowa Iowa City, Iowa 52242

Received August 21, 1989

η^2-Acyl ligands are common products from carbonylation of early-transition-metal, lanthanide, and actinide alkyls[1] and have been studied primarily from a synthetic or structural rather than a reactivity perspective. Reactions of η^2-acyls include insertion into aryl C-H bonds[2-4] and conversion into metal-bound enolates,[5-7] ketenes,[8] carboxylates,[9] ketones,[10] and mononuclear and dinuclear enediolates.[11] There are interesting reports of η^2-acyl C-O bond cleavage, including formal O atom abstraction to generate metal carbynes,[12] CO deoxygenation/cyclopentadiene synthesis following CO insertion/ring expansion into metallacyclo-3-pentene complexes[13] (which may proceed through an acyl intermediate), and generation of hexaalkylbenzenes from a $(C_5Me_5)_2Ti(III)$ acyl upon reaction with $Cp_2Mo_2(CO)_6$.[14] Our interests in mid-valent, mono(η-C_5R_5) early-metal chemistry[15,16] and in the comparative structure/reactivity of organometallic functional groups in complexes with different metal valencies led us to examine whether an electronically unsaturated η^2-acyl complex would deinsert, rearrange to a ketene hydride,[17] have altered η^2-interaction and reactivity, or undergo structural rearrangement upon reduction. We have discovered an example of the latter, specifically that η^2-acyl reduction can lead to deoxygenative coupling with a cyclopentadienyl C_{ring}-C_{ring} bond.

The η^2-acyl complex (η-C_5Me_4R)Ta[C(O)CH_2CMe_3]Cl_3 (**1**; R = Me, Et),[4,18,19] which is to our knowledge the most structurally distorted[18b] transition-metal η^2-acyl, is reduced by Mg, Na/Hg, K/Hg, Zn, or sodium naphthalenide in a variety of solvents to a dark orange solution, from which the arene $C_6Me_5(CH_2CMe_3)$ can be sublimed after centrifugation or filtration (eq 1). The

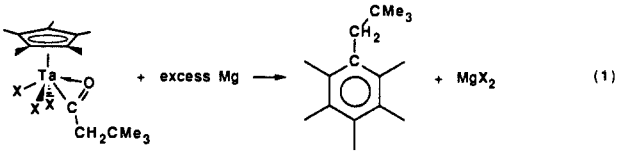

(1)

highest yields (61% isolated, 75% GC based on **1**) are obtained with 4 equiv of Mg in Et_2O. The arene GC yield decreases to 50% with 2 equiv of Mg or 1, 2, or 4 equiv of Na/Hg, while 0.5 equiv of Na/Hg resulted in ca. 23% GC yield. The other reductants behaved similarly but produced lower arene yields. The arene was identified by ^1H and ^{13}C NMR spectroscopy, mass spectrometry,[20] and X-ray diffraction.

The tantalum-containing product(s) are presently unidentified because of the difficulty in direct separation from byproducts or separation via derivatization. Characterization of the tantalum product(s) has been hampered by a concurrent, slow ($\tau_{1/2}$ = 1-2 days in the absence of reductant) decomposition of the starting

(1) Durfee, L. D.; Rothwell, I. P. *Chem. Rev.* **1988**, *88*, 1059-1079.
(2) Evans, W. J.; Hughes, L. A.; Drummond, D. K.; Zhang, H.; Atwood, J. L. *J. Am. Chem. Soc.* **1986**, *108*, 1722-1723.
(3) Fanwick, P. E.; Kobriger, L. M.; McMullen, A. K.; Rothwell, I. P. *J. Am. Chem. Soc.* **1986**, *108*, 8095-8097.
(4) Arnold, J.; Tilley, T. D.; Rheingold, A. L.; Geib, S. J.; Arif, A. M. *J. Am. Chem. Soc.* **1989**, *111*, 149-164.
(5) Fagan, P. J.; Manriquez, J. M.; Marks, T. J.; Day, V. W.; Vollmer, S. H.; Day, C. S. *J. Am. Chem. Soc.* **1980**, *102*, 5393-5396.
(6) Maata, E. A.; Marks, T. J. *J. Am. Chem. Soc.* **1981**, *103*, 3576-3578.
(7) (a) Theopold, K. H.; Becker, P. N.; Bergman, R. G. *J. Am. Chem. Soc.* **1982**, *104*, 5250-5252. (b) Liebeskind, L. S.; Welker, M. E. *Organometallics* **1983**, *2*, 194-195 and references therein.
(8) (a) Straus, D. A.; Grubbs, R. H. *J. Am. Chem. Soc.* **1982**, *104*, 5499-5500. (b) Moore, E. J.; Straus, D. A.; Armantrout, J.; Santarsiero, B. D.; Grubbs, R. H.; Bercaw, J. E. *J. Am. Chem. Soc.* **1983**, *105*, 2068-2070. (c) Messerle, L. Ph.D. Thesis, Massachusetts Institute of Technology, Cambridge, MA, 1979.
(9) Bonnesen, P. V.; Yau, P. K. L.; Hersh, W. H. *Organometallics* **1987**, *6*, 1587-1590.
(10) (a) Waymouth, R. M.; Clauser, K. R.; Grubbs, R. H. *J. Am. Chem. Soc.* **1986**, *108*, 6385-6387. (b) Waymouth, R. M.; Grubbs, R. H. *Organometallics* **1988**, *7*, 1631-1635. (c) Martin, B. D.; Matchett, S. A.; Norton, J. R.; Anderson, O. P. *J. Am. Chem. Soc.* **1985**, *107*, 7952-7959.
(11) Wolczanski, P. T.; Bercaw, J. E. *Acc. Chem. Res.* **1980**, *13*, 121-127.
(12) (a) McDermott, G. A.; Dorries, A. M.; Mayr, A. *Organometallics* **1987**, *6*, 925-931. (b) Brower, D. C.; Stoll, M.; Templeton, J. L. *Organometallics* **1989**, *8*, 2786-2792.
(13) (a) Blenkers, J.; de Liefde Meijer, H. J.; Teuben, J. H. *Organometallics* **1983**, *2*, 1483-1484. (b) Hessen, B.; Blenkers, J.; Teuben, J. H.; Helgesson, G.; Jagner, S. *Organometallics* **1989**, *8*, 2809-2812.
(14) De Boer, E. J. M.; De With, J. *J. Organomet. Chem.* **1987**, *320*, 289-293.
(15) (a) Ting, C.; Messerle, L. *J. Am. Chem. Soc.* **1987**, *109*, 6506-6508. (b) Ting, C.; Messerle, L. *J. Am. Chem. Soc.* **1989**, *111*, 3449-3450. (c) Ting, C.; Messerle, L. *Inorg. Chem.* **1989**, *28*, 171-173.
(16) Messerle, L. *Chem. Rev.* **1988**, *88*, 1229-1254.
(17) Bruno, J. W.; Fermin, M. C.; Halfon, S. E.; Schulte, G. K. *J. Am. Chem. Soc.* **1989**, *111*, 8738-8740.
(18) (a) Meyer, T. Y.; Messerle, L. Abstracts, Third Chemical Congress of North America, Toronto, Canada, June 9, 1988; INOR 583. (b) Meyer, T. Y.; Garner, L. R.; Baenziger, N. C.; Messerle, L. *Inorg. Chem.*, in press.
(19) Rocklage, S. M. Ph.D. Thesis, Massachusetts Institute of Technology, Cambridge, MA, 1982, pp 170-176.
(20) (a) ^1H NMR (δ, C_6D_6): 0.93 (s, 9, CMe_3), 2.12 (s, 9, arene Me, Me'), 2.20 (s, 6, arene Me''), 2.80 (s, 2, CH_2). ^{13}C NMR (δ, $\{^1H\}$): 16.9, 17.2, 19.3 (arene Me's), 30.4 (CMe_3), 34.6 (CMe_3), 41.3 (CH_2), 132.1, 132.4, 133.2 (arene-ring carbons), 133.9 (CCH_2CMe_3). MS (m/e): 218 (P^+), 161 ($P^+ - CMe_3$). (b) The ^1H and ^{13}C NMR data match the data reported in the literature.[18c] (c) Hallden-Abberton, M.; Engelman, C.; Fraenkel, G. *J. Org. Chem.* **1981**, *46*, 538-546.

0002-7863/90/1512-4564$02.50/0